https://doi.org/10.15302/frontphys.2025.044210
RESEARCH ARTICLE

Manipulation of valley polarization and topology in monolayer $MoSnC_2S_6$ and $MoPbGe_2Te_6$

Xianjuan He [1], Wenzhe Zhou [1,†] Zhenzhen Wan[1,2], Yating Li [1], Chuyu Li [1], Fangping Ouyang [1,2,3,‡]

[1]School of Physics, Institute of Quantum Physics, Hunan Key Laboratory for Super-Microstructure and Ultrafast Process, and Hunan Key Laboratory of Nanophononics and Devices, Central South University, Changsha 410083, China

[2]School of Physics and Technology, State Key Laboratory of Chemistry and Utilization of Carbon-Based Energy Resources, Xinjiang University, Urumqi 830046, China

[3]State Key Laboratory of Powder Metallurgy, and Powder Metallurgy Research Institute, Central South University, Changsha 410083, China

Corresponding authors. E-mail: [†]csuzwz22@csu.edu.cn, [‡]ouyangfp06@tsinghua.org.cn

Received September 26, 2024; accepted January 16, 2025

Supporting Information

Table S1 The nearest Heisenberg magnetic exchange interaction coefficients, MAE and T_C.

Systems	J (meV)	MAE (meV)	T_C (K)	Systems	J (meV)	MAE (meV)	T_C (K)
$MoGeC_2S_6$	34.539	0.423	439	$WGeC_2S_6$	24.061	1.735	312.5
$MoGeSi_2S_6$	30.024	-0.406	390	$WGeSi_2S_6$	22.468	-7.455	309
$MoPbGe_2S_6$	21.692	-0.501	277.5	$WPbGe_2S_6$	16.551	-8.028	232
$MoPbSi_2S_6$	15.234	2.565	211	$WPbSi_2S_6$	12.388	17.031	225
$MoSnC_2S_6$	35.255	0.414	460	$WSnC_2S_6$	25.261	2.967	340.5
$MoSnGe_2S_6$	36.292	-0.251	470.5	$WSnGe_2S_6$	27.057	-4.594	358
$MoSnSi_2S_6$	30.418	-0.337	392	$WSnSi_2S_6$	27.384	-6.487	372
$MoGeC_2Se_6$	35.703	0.435	462	$WGeC_2Se_6$	25.891	4.414	358
$MoGeSi_2Se_6$	32.437	-0.382	411	$WGeSi_2Se_6$	27.762	-5.67	372
$MoPbGe_2Se_6$	25.889	-0.448	333.5	$WPbGe_2Se_6$	21.882	-4.246	291.5
$MoPbSi_2Se_6$	20.089	1.571	260	$WPbSi_2Se_6$	17.182	7.718	263.5
$MoSnC_2Se_6$	34.653	0.646	448	$WSnC_2Se_6$	24.928	5.91	354.5
$MoSnGe_2Se_6$	37.059	-0.109	479.5	$WSnGe_2Se_6$	32.245	-2.961	411
$MoSnSi_2Se_6$	33.068	-0.055	418	$WSnSi_2Se_6$	31.879	-3.672	418
$MoGeC_2Te_6$	30.839	-4.188	404	$WGeC_2Te_6$	21.909	0.482	277.5
$MoGeSi_2Te_6$	31.504	-0.673	393.5	$WGeSi_2Te_6$	31.141	-1.817	393.5

$MoPbGe_2Te_6$	25.127	-0.977	319.5	$WPbGe_2Te_6$	26.154	-0.145	333.5
$MoPbSi_2Te_6$	21.726	1.403	277.5	$WPbSi_2Te_6$	22.316	4.333	312.5
$MoSnC_2Te_6$	27.099	-2.835	351	$WSnC_2Te_6$	12.569	-0.94	158.5
$MoSnGe_2Te_6$	35.334	-0.188	458.5	$WSnGe_2Te_6$	35.062	0.22	439
$MoSnSi_2Te_6$	33.247	-0.067	427	$WSnSi_2Te_6$	34.412	0.678	439

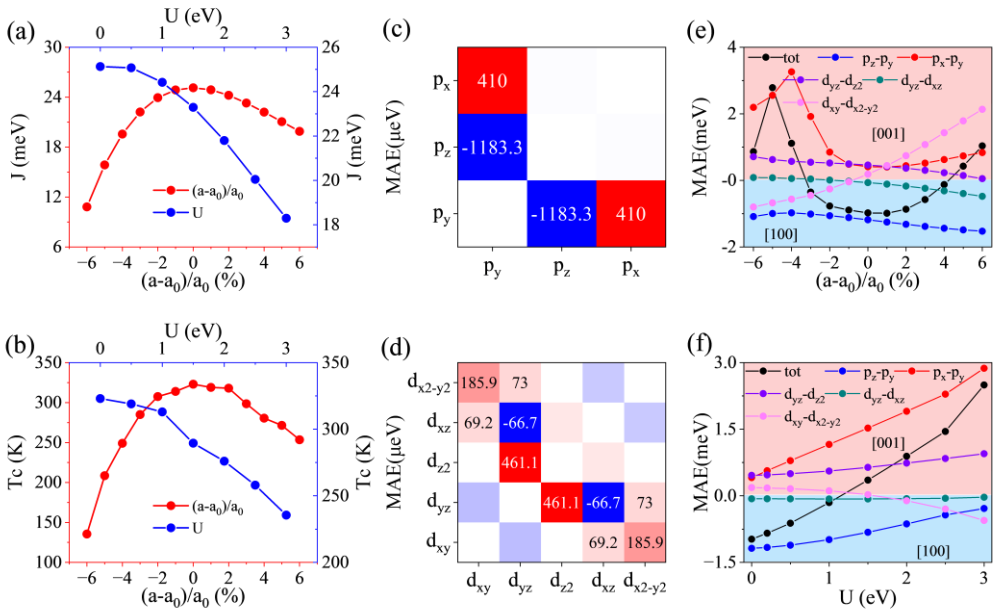

Fig. S1 For $MoPbGe_2Te_6$, **(a)** J and **(b)** T_C as a function of biaxial strain and U. Orbital-resolved MAE of **(c)** p orbitals and **(d)** d orbitals. Total MAE and orbital donations as a function of **(e)** biaxial strain and **(f)** U.

Fig. S1(a) shows the variation of J with biaxial strain and U. J of $MoPbGe_2Te_6$ is 25.13 meV. As strain reaches to -6% and 6%, J decreases to 10.81 and 19.89 meV, respectively. As U increases to 3 eV, J decreases to 18.29 meV.

To clearly comprehend the physical mechanism of MAE of $MoPbGe_2Te_6$, the orbital-resolved MAE of p and d orbitals are displayed in **Fig. S1**(c) and **Fig. S1**(d). The p_x/p_y orbitals primarily contribute to the in-plane MAE of -1183.3 μeV. Meanwhile, the d_{yz}/d_z^2 orbitals, as well as the p_x/p_y orbitals, primarily contribute to the out-of-plane MAE of 461.1 μeV and 410 μeV, respectively. Spontaneous valley polarization occurs only when the easy axis of magnetization is along the z axis. Therefore, biaxial strain and U are used to regulate MAE. As **Fig. S1**(e) shows, MAE increases from 0.863 meV to 2.784 meV as strain varies from -6% to -5%, and then increases to 1.112 meV as strain is -4%. From -3% to 4% strain, MAE is negative, indicating in-plane easy magnetization axis. From 5% to 6% strain, the value of MAE becomes positive. The p_x/p_y orbitals always donate to the out-of-plane MAE, while the p_y/p_z orbitals always donate to the in-plane MAE.

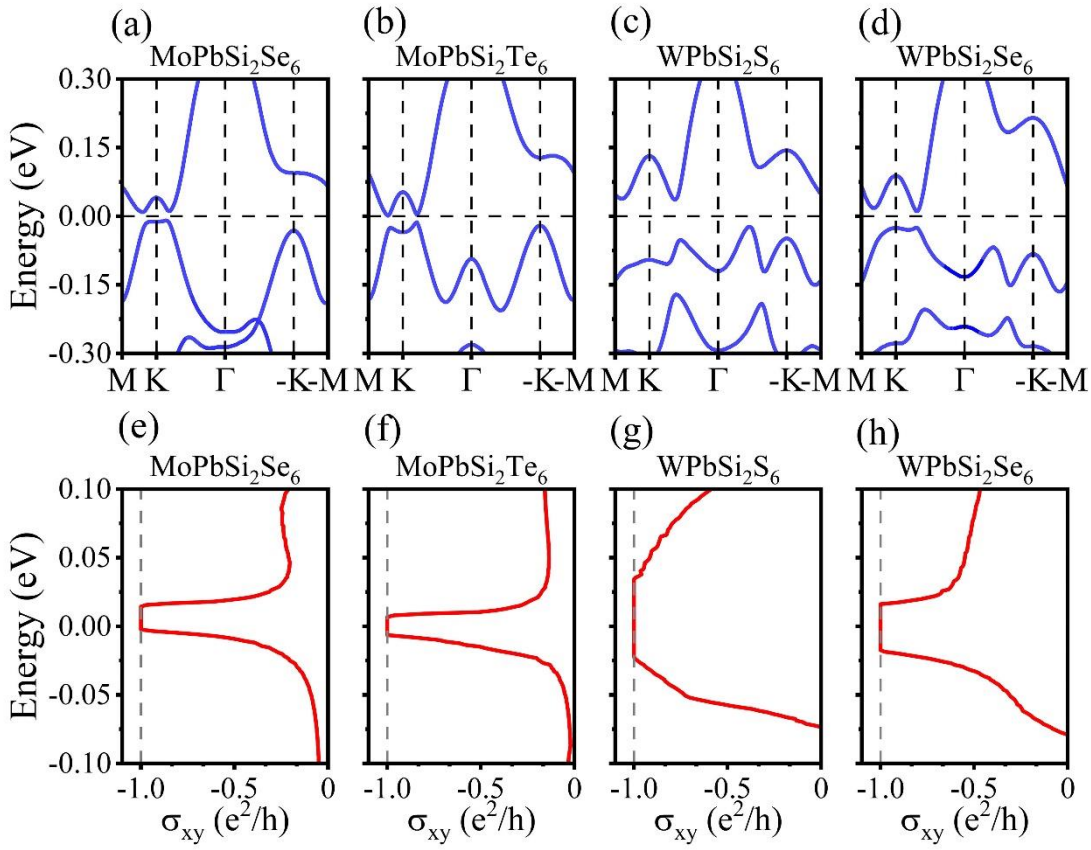

Fig. S2 Band of **(a)** $MoPbSi_2Se_6$, **(b)** $MoPbSi_2Te_6$, **(c)** $WPbSi_2S_6$, **(d)** $WPbSi_2Se_6$ when SOC is considered. Anomalous Hall conductivity of **(e)** $MoPbSi_2Se_6$, **(f)** $MoPbSi_2Te_6$, **(g)** $WPbSi_2S_6$, **(h)** $WPbSi_2Se_6$ when SOC is considered.

There are four systems possess intrinsic topological phase without manipulation. As shown in **Fig. S2**, the AHC of $MoPbSi_2Se_6$, $MoPbSi_2Te_6$, $WPbSi_2S_6$ and $WPbSi_2Se_6$ exhibit plateaus near the Fermi level, proving the quantum anomalous Hall (QAH) effect. And the plateaus are 16.6, 13.1, 56.2 and 33.5 meV, respectively. And the Chern number C = -1.

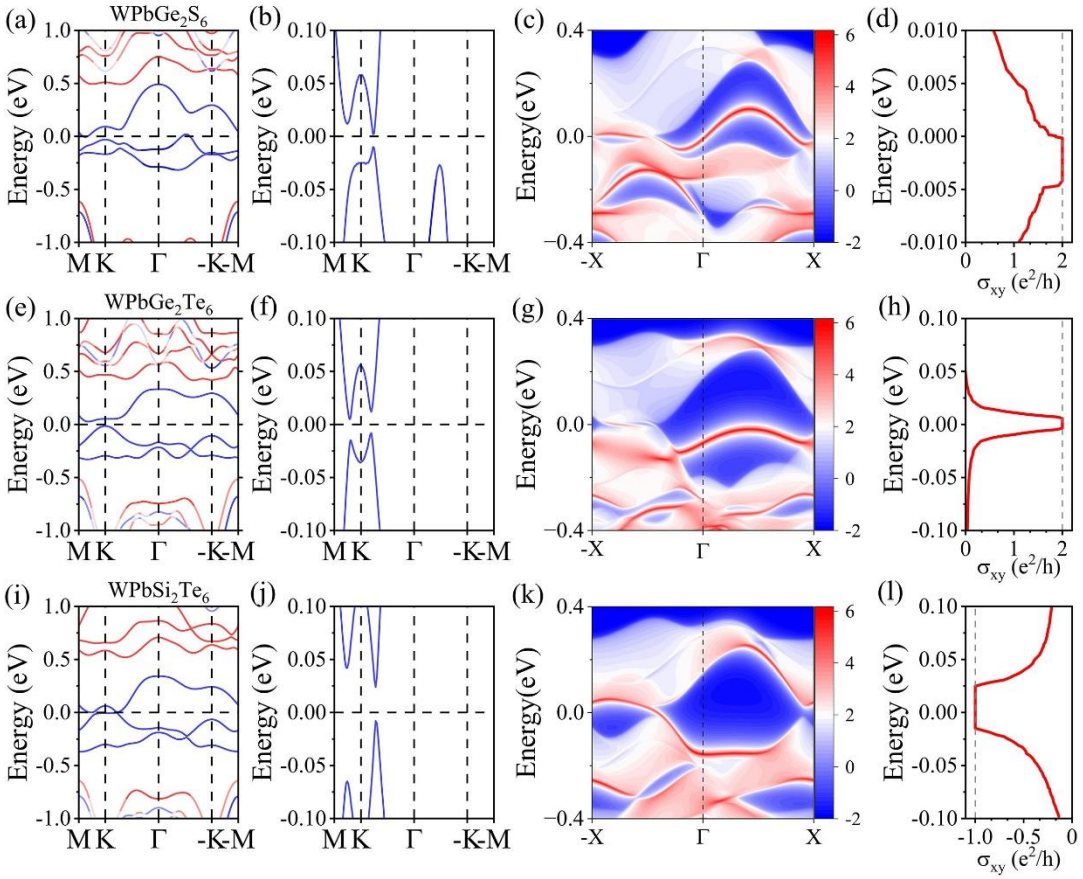

Fig. S3 The spin-polarized band structures with SOC of **(a)** $WPbGe_2S_6$, **(e)** $WPbGe_2Te_6$ and **(i)** $WPbSi_2Te_6$, and the spin-polarized band structures with SOC of **(b)** $WPbGe_2S_6$, **(f)** $WPbGe_2Te_6$ and **(j)** $WPbSi_2Te_6$ when U is 2 eV. The blue and red lines represent spin-up and spin-down channels, respectively. The topological edge states (marked with red) calculated along the (010) direction of **(c)** $WPbGe_2S_6$ (right side), **(g)** $WPbGe_2Te_6$ (right side) and **(k)** $WPbSi_2Te_6$ (left side) and anomalous Hall conductivity of **(d)** $WPbGe_2S_6$, **(h)** $WPbGe_2Te_6$ and **(l)** $WPbSi_2Te_6$ with SOC when U is 2 eV.

Apart from systems that exhibit topological properties in their intrinsic states, some systems that do not have topological properties in their intrinsic states can exhibit topological properties under the regulation of the U value. Besides $MoPbGe_2Te_6$, $WPbGe_2S_6$, $WPbGe_2Te_6$ and $WPbSi_2Te_6$ exhibit the QAH effect under the regulation of the U. As shown in **Fig. S3**, $WPbGe_2S_6$ is metallic phase with spin-up channels crossing the Fermi level. However, band reverses around K point when U is 2 eV. **Fig. S3**(c) displays the edgestate of $WPbGe_2S_6$. It is clearly that there are two edge states connecting the valence band (VB) and conduction band (CB). The anomalous Hall conductivity (AHC) also exhibits a plateau near the Fermi level, and the Chern number $C = 2$, demonstrating QAH effect occurs when U is 2 eV. $WPbGe_2Te_6$ is semiconductor, and the spin-up and spin-down channels are fully polarized near the Fermi level, and electronic states are fully donated by spin-up states. Band reversion occurs around K point when U is 2 eV as shown in **Fig. S3**(f). Two chiral edge states connect the CB and VB. Differs from $WPbGe_2S_6$ and $WPbGe_2Te_6$, the band of $WPbSi_2Te_6$ reverses around K point when U is 0 eV. However, the bandgap is closed and there is no plateau in AHC. Therefore, it is possible to achieve a topological state by opening the bandgap through certain manipulation.

The DFT calculations demonstrate that $WPbSi_2Te_6$ exhibits topological properties when U is 2 eV, the chern number C = -1. As displayed in **Fig. S3**(j), a bandgap of 44 meV near K point is opened when U is 2 eV. A chiral edgestate is present and connects the CB and VB, resulting in the motion of Bloch electrons for Hall conductivity. The AHC is also calculated, as shown in **Fig. S3**(l). There is a plateau near the Fermi level, demonstrating that QAH phase is achieved when U is 2 eV.